CASE SERIES

First report case with negative genetic study (array CGH, exome sequencing) in patients with vertical transmission of Zika virus infection and associated brain abnormalities

Estephania Candelo[1,2]
Gabriela Caicedo[1]
Fernando Rosso[3]
Adriana Ballesteros[4]
Jaime Orrego[4]
Luis Escobar[5]
Pablo Lapunzina[6,7]
Julián Nevado[6,7]
Harry Pachajoa[1,8]

[1]Center for Research on Congenital Anomalies and Rare Diseases (CIACER), Department of Basic Medical Sciences, Universidad Icesi, Cali, Colombia; [2]MSc Biomaterials and Tissues Engineering and Genetics of Human Diseases, University College London, London, UK; [3]Infectology Department, Fundación Valle del Lili, Cali, Colombia; [4]Neonatal Department, Fundacion Valle del Lili, Cali, Colombia; [5]Pathology Department, Fundacion Valle del Lili, Cali, Colombia; [6]Instituto de Genética Médica y Molecular (INGEMM), IdiPAZ, Hospital Universitario La Paz, Madrid, 28046, Spain; [7]CIBER de Enfermedades Raras (CIBERER), Madrid, ISCIII, Spain; [8]Genetics Department, Fundacion Valle del Lili, Cali, Colombia

Correspondence: Harry Pachajoa
Centro de Investigaciones en Anomalías, Congénitas y Enfermedades Raras, Universidad ICESI, Calle, 18 N° 122-135, Cali, Colombia
Tel +57 2 555 2334
Fax +57 216 368 0564
Email hmpachajoa@icesi.edu.co

Introduction: Zika virus (ZIKV) is a little-known emerging mosquito-borne flavivirus. The perinatal ZIKV infection was associated with birth defects during the Brazilian outbreak. There was an increased risk of intrauterine transmission of the virus and a marked increase in the number of newborns with microcephaly. We report on two such cases.

Case Report: The first case was a 25-year-old pregnant woman from Colombia who became acutely ill with general symptoms during the tenth week of gestation, followed by severe generalized itching and maculopapular rash for approximately five days. This case was reported during the epidemic stage of the ZIKV infection in Colombia. At 23.3 gestational weeks, ultrasonography showed abnormal intracranial anatomy with cerebral ventriculomegaly, microcephaly, and parenchymal calcification. Given the grave prognosis, the patient elected to terminate the pregnancy at 25 gestational weeks. The second case was a 24-year-old pregnant woman who became acutely ill during the 17th week of gestation, which corresponded with the ZIKV epidemic in Colombia. At 30.5 gestational weeks, ultrasonography showed isolated fetal cerebral ventriculomegaly. We detected ZIKV in the amniotic fluid; however, the virus was not detected in the urine or serum of the mother or fetus. Tests for dengue virus, chikungunya virus, Toxoplasma gondii, rubella virus, cytomegalovirus, herpes simplex virus, HIV, hepatitis B and C, and parvovirus B19 were all negative. Different samples obtained from the placenta, amniotic liquid, and cerebrospinal fluid were positive for viral isolation of ZIKV RNA using TaqMan RT-PCR. Additionally, the parents and fetuses were tested for genetic diseases using whole exome sequencing and array CGH to rule out possible genetic syndromes that produce these congenital abnormalities.

Conclusion: These were the first cases in Colombia to show early vertical transmission of ZIKV and the first cases associated with congenital cerebral abnormalities in which molecular, infectious, and genomic tests were performed.

Keywords: Colombia, microcephaly, whole exome sequencing, Zika virus infection, vertical transmission, brain abnormalities

Introduction

Zika virus (ZIKV) is an emerging arthropod-borne virus of the Flaviviridae family.[1] This RNA virus contains 10,794 nucleotides that encode 3,419 amino acids.[2] It is transmitted by the Aedes mosquitoes, as are the dengue and chikungunya viruses. It was first isolated in April 1947, in a *Rhesus macaque* in a Zika forest in Uganda.[3,4] At the time, there was no initial indication that the virus caused disease in humans.

The first human case was reported in Nigeria in 1952.[3] ZIKV was only believed to cause sporadic benign human infections in Africa and Asia until the recent occurrence of three significant outbreaks.[5] The first occurred on the island of Yap, Micronesia, in 2007, when a massive epidemic was reported and nearly 75% of the population was infected with the virus.[6] The second and largest outbreak was in French Polynesia between 2013 and 2014.[3,5] The virus has since spread throughout the Americas, with original cases identified in several countries.

The first ZIKV cases in the Americas were reported on Easter Island (Chile) where 89 samples were obtained from patients with suspected ZIKV infection.[7] Fifty-one of those samples had positive reverse-transcriptase-polymerase-chain-reaction (RT-PCR) for ZIKV. From there, the virus spread throughout the Pacific, reaching northeastern Brazil in 2015.[1] Between April and November 2015, 18 of the 27 Brazilian states reported ZIKV autochthonous cases.[8] In December 2015, the Ministry of Health in Brazil reported up to 1,300,000 suspected cases of the ZIKV.[8] By January 2016, there were reported cases of local transmission in Puerto Rico and 19 other countries or territories in the Americas.[3] In 2016 in Colombia, 31,555 cases of ZIKV infection were reported with 25,950 confirmed by clinical manifestation, 4,101 suspected cases, and 1,504 laboratory-confirmed cases. Colombia had the second highest number of people infected with ZIKV, surpassed only by Brazil.[9,10] At the end of 2016, the causal relationship between ZIKV and congenital abnormalities was recognized. This event changed public health history.[11] Unfortunately, the prevalence of ZIKV infection in endemic countries is unknown. However, seroprevalence surveys indicate a seroconversion range between 1% and 50% in the population.[12] Current reports and accumulating data have shown that ZIKV in endemic areas has teratogenic effects for an extended period, which had not been recognized before the Brazil outbreak. This assumption was made based on the cases of two older children from the United States (US), who displayed a consistent phenotype similar to that of Zika congenital syndrome. In both cases, the mothers reported Zika symptoms in the first and second term of pregnancy and laboratory-confirmed ZIKV was reported.[13]

In the US, approximately 10% of pregnancies with laboratory-confirmed ZIKV infection have resulted in congenital syndrome. The absolute risks have been estimated as 15% when the infection is confirmed in the first trimester, gradually decreasing as the pregnancy becomes closer to term.[11] However, the overall risk of birth defects associated with ZIKV was found to be higher than that for mothers with no exposure to ZIKV (3.6–12.7%) over all three trimesters.[11] Previous studies have demonstrated that the risk of congenital neurologic defects ranges from 6 to 42%.[14] According to a prospective cohort in the French Territories, neurologic and ocular defects related to ZIKV infection were observed in fetuses and infants, with an incidence of approximately 7% (95% CI: 5–9.5%). As other studies have reported, birth defects in infants and fetuses were more frequent in the early stages of pregnancy: 12.7% during the first trimester, 3.6% during the second trimester, and 5.3% during the third trimester (P=0.001).[14]

The prevalence of microcephaly from 1982 to 2013 (before the ZIKV outbreak) ranged between 0.3 and 31 cases per 100,000 live births, with an average of 1.8 cases (95% CI 1.7–1.8) per 100,000 live births. However, the prevalence of microcephaly after ZIKV introduction is unknown.[15] The ZIKV epidemic in Colombian territories began in August 2015 and laboratory evidence showed positive samples by October 2015. By April 2016, there were 65,726 suspected cases of ZIKV infection reported in Colombia, but only 4% of them were confirmed using RT-PCR assay.[10] A total of 11,944 pregnant women reported symptoms and ZIKV was confirmed in 12% of these women. From this suspected population, 50 infants displayed possible microcephaly. However, of that number, only four infants had birth defects including brain abnormalities and hearing abnormalities related to ZIKV congenital infection.[10] In this case series, we present the first case of Zika congenital syndrome with complete molecular, microbiological, and genetic assessment.

Materials and methods
First case report
In June 2016, a 25-year-old woman, who was pregnant for the second time, carried a female fetus that displayed multiple congenital abnormalities. The pregnancy started in December 2015 and was without abnormalities until February 2016. At 10 weeks of pregnancy, the mother presented rash in the face and superior limbs, conjunctival hyperemia, arthralgia, headache, myalgia, and fever. A ZIKV infection was suspected and RT-PCR was performed, which showed a positive result at 10 weeks of gestation. As a result, a ZIKV congenital infection was

suspected and continuous ultrasonography monitoring was performed from weeks 10 to 17, with no evidence of birth defects observed. As part of the prenatal care, TORCH testing was performed, and the most prevalent congenital infections were eliminated as causal factors including toxoplasmosis, syphilis, HIV, rubella, cytomegalovirus, hepatitis B, herpes virus 1 and 2, and parvovirus B19 (Table 1).

At 23.3 weeks of gestation, the first brain abnormalities were observed. Ultrasonography showed asymmetric fetal growth during pregnancy, cephalic perimeter and biparietal diameter below the 5th percentile, intracranial calcifications, and ventriculomegaly (atrial diameter of 21.1 mm) without other structural malformations. Combined with the previous positive Zika RT-PCR and ultrasonography findings, congenital ZIKV syndrome was diagnosed. Because of the poor fetal prognosis, the parents decided to terminate the pregnancy following National Legislation and Medical Team approval. When the fetus was born, the

Table 1 Molecular and viral diagnosis. Results of different tests for possible perinatal infections associated with congenital abnormalities according to the different trimesters

Test	First case			Second case		
	First trimester	**Second trimester**	**Third trimester**	**First trimester**	**Second trimester**	**Third trimester**
ZIKV positive results						
In blood and amniotic liquid		Positive	Positive			
In blood only	Positive	Positive	Positive			Negative
In amniotic liquid only		Positive	Positive			Positive
TORCH						
Toxoplasmosis						
Toxoplasma IgG	Positive	Positive	Positive	Negative	Negative	Negative
Toxoplasma IgM	Negative	Negative	Negative	Negative	Negative	Negative
Syphilis						
RPR Serology	Negative	Negative	Negative	Negative	Negative	Negative
HIV	Negative	Negative	Negative	Negative	Negative	Negative
Rubella						
Rubeola IgG	Positive	Positive	Positive	Positive	Positive	Positive
Rubeola IgM	Negative	Negative	Negative	Negative	Negative	Negative
CMV						
CMV IgG		Negative	Negative			Positive
CMV IgM		Negative	Negative			Negative
Dengue						
Dengue IgG			Negative			Negative
Dengue IgM			Negative			Negative
Chikungunya						
Chikungunya IgG			Negative			Negative
Chikungunya			Negative			Negative
Parvovirus B19			Negative			Negative
Herpes simplex 1 and 2			Negative			Negative
Hepatitis B antibodies HBS	Negative	Negative	Negative	Negative	Negative	Negative
Karyotype	46, XX			46, XY		

Abbreviations: ZIKV, Zika virus; RA, retinoic acid.

only morphological finding was microcephaly. An entire genetic assessment was performed on the fetus, including an assessment of inheritance genetic disorders; an autopsy was also performed.

Autopsy and central nervous system (CNS) examination

An autopsy of the fetus was performed the same day as the termination of pregnancy. All the samples were fixed in 10% buffered formalin and embedded in paraffin. Fresh tissue samples were collected for the microbiological analysis. A section of all tissue samples was stained with hematoxylin and eosin, following CDC protocol and a previous report.[16] (Figures 1 and 2)

Second case report

The second case was a 24-year-old pregnant woman from Colombia. During the 17th week of gestation, she became acutely ill, with fatigue that was followed by severe generalized itching and maculopapular rash for seven days, associated with anorexia, nausea, vomiting, and headache. The illness continued for the following five days, when the generalized rash disappeared. Her close familial group (her partner, mother, and sister) were concomitantly reporting similar symptoms. Since there was a ZIKV outbreak in Colombia, infection with the virus or another arthropod-

transmitted virus was suspected, but no virological or serological diagnostic testing was performed. Multiple fetal ultrasonographies were performed at 20, 24, 30, 31, and 34 weeks of gestation (4, 8, 14, 15, and 18 weeks after the resolution of symptoms) (Figure 3A–C). Until 30 weeks of gestation, the fetal ultrasonography evaluations showed normal anatomy and fetal growth with no birth defects. No evidence of microcephaly or intracranial calcifications was observed until 30.3 weeks of gestation. However, there was an increase in the fetal atrial diameter to 19.6 mm at 30 gestational weeks (Figure 3A–C). This finding was considered indicative of severely isolated ventriculomegaly because the fetus had no other evident abnormalities. After this finding, a virologic test was performed in the amniotic fluid, which tested positive for ZIKV.

The fetal ultrasonography at 30 gestational weeks showed abnormal intracranial ventricular dilatation. Medium line elements were conserved, and the cavum septum pellucidum was not visualized. Moderate communicable ventriculomegaly was observed. The head circumference measured in the 85th percentile for gestational age. Fetal ultrasonographies were also performed at 31 and 34 weeks of gestation and showed dilatation and enlarged posterior horns of the lateral ventricles; the third ventricle had a transverse diameter at the level of the atria that measured 16.2 mm (average measurement at gestational
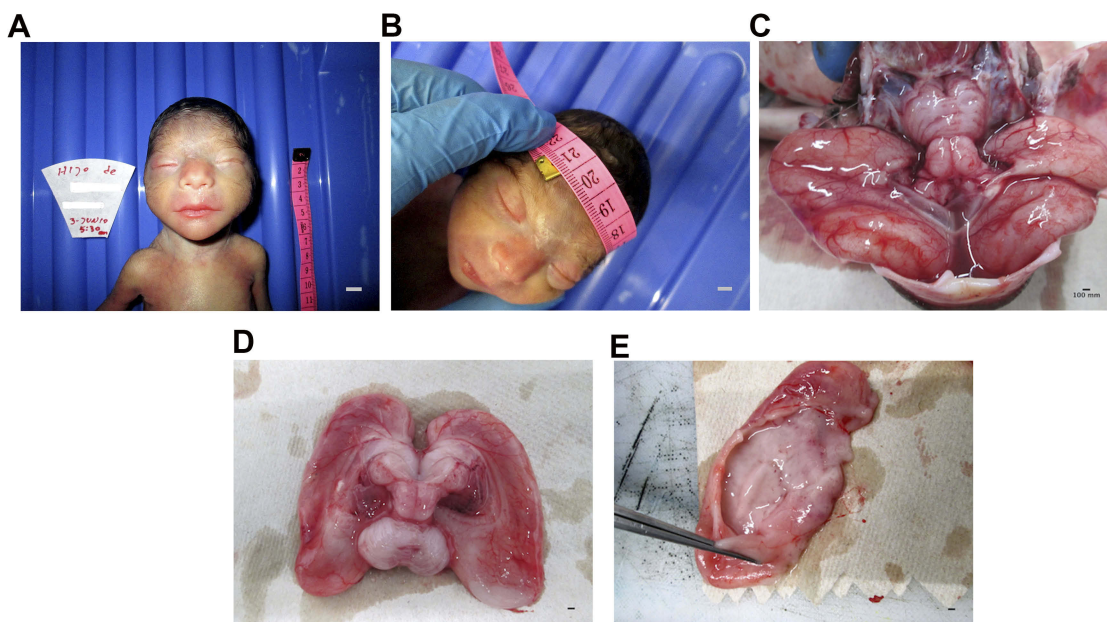

Figure 1 In postmortem macroscopic analysis of samples obtained from the fetus autopsy. (**A**) Female proband with Zika congenital syndrome without other congenital abnormalities apart from brain abnormalities and microcephaly. (**B**) Head circumference of 20 cm (less than −2 SD). (**C**) Absence of the corpus callosum. (**D**) Hydrocephalus of the lateral ventricle. (**E**) Near-complete agyria. Scale bar is shown on the bottom right of each panel. Scale bar 1.03 cm/pixel in all the pictures.
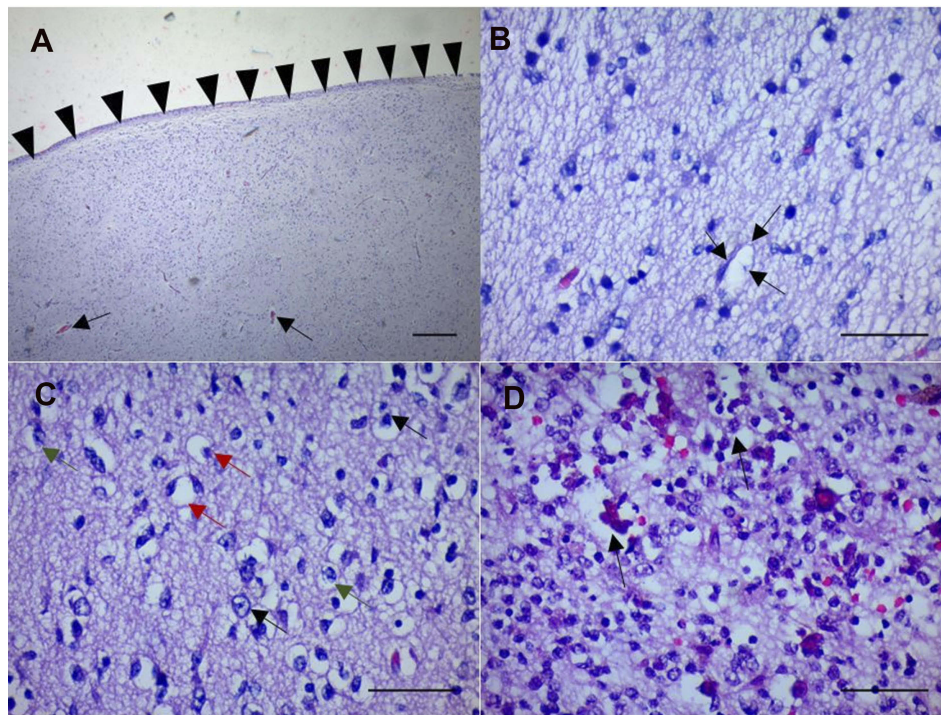
Figure 2 In postmortem microscopic analysis of samples obtained from the fetus autopsy. (**A**) The sulci have almost disappeared, making the brain surface smooth, which is highlighted in the image by the small triangles and the arrows showing intensive gliosis with Rosenthal fibers. (**B**) Neural loosening due to the neural injury in the surroundings. It is possible to see some inflammatory cells and neural vacuolation (arrows). (**C**) Arrow shows non-specific reactive changes with astrocyte proliferation, gliosis, and edema (astrogliosis) as part of the glial scaring process. Neural vacuolation and degenerate axons devoid of myelin sheath (Wallerian degeneration, red arrows) and macrophages occupying the space of a former axon (green arrows). (**D**) Microcalcifications (arrows) and gliosis. Hematoxylin and eosin staining was used to visualize the previous panels. Scale bar is shown on the bottom right of each panel. Scale bar is shown on the bottom right of each panel. Scale bar for figure A 1.03 um/pixel and figures B, C and D 0.518 um/pixel.

age, 6.73 mm [range, 5.7–7.7]) (Figure 3A–C). The fourth ventricle and the choroid plexus were healthy, with no evidence of hemorrhage. No focal destructive lesions were identified within the cerebral cortex or white matter.

At 31 weeks of gestation, the presence of flavivirus in the amniotic liquid was detected in the RT-PCR assay. This finding was confirmed with a specific ZIKV quantitative RT-PCR assay. The National Health Institute in Colombia (NHI) reported serological and virologic evidence of infection at 36 weeks of gestation, with RT-PCR positivity in the amniotic liquid for ZIKV. At 37 weeks of gestation, the baby was born through vaginal delivery without complications and was evaluated by an expert neonatologist. The baby was male with a weight of 2,629 g (p10), a height of 48 cm (p50-10), and a head circumference of 32 cm (p10) (average measurement at gestational age). A brain tomography showed hydrocephalus (Figure 3D).

The presence of other possible perinatal infections was evaluated including Toxoplasma gondii, rubella virus, cytomegalovirus, herpes simplex virus, HIV, hepatitis B and C, and parvovirus B19 (STORCH); however, negative results were reported for these infections (Table 1).

Sample collection

Following NIH recommendations, amniocentesis was performed at 23.3 and 31 gestational weeks, respectively, to investigate the cause of the multiple brain abnormalities. Ultrasound-guided transabdominal amniocentesis was performed and approximately 5 ml of amniotic fluid was aspirated and immediately stored at −80 °C. An additional sample was obtained from the cerebrospinal liquid when the infant was born.

Viral detection

Molecular detection of ZIKV in the amniotic liquid and brain-spinal liquid was performed by the NIH of the Colombian Government using the SuperScript III Platinum One-Step RT-PCR system (Invitrogen). The NIH used the oligonucleotides ZIKV 1087/ZIKV 1163 and ZIKV 1108-FAM, following the Lanciotti protocol.[6] For hybridization and extension, ABI7500 equipment was used (ThermoFisher Scientific).[10]

We tested the samples obtained from the patient and the newborn, as well as samples from viral isolation trials
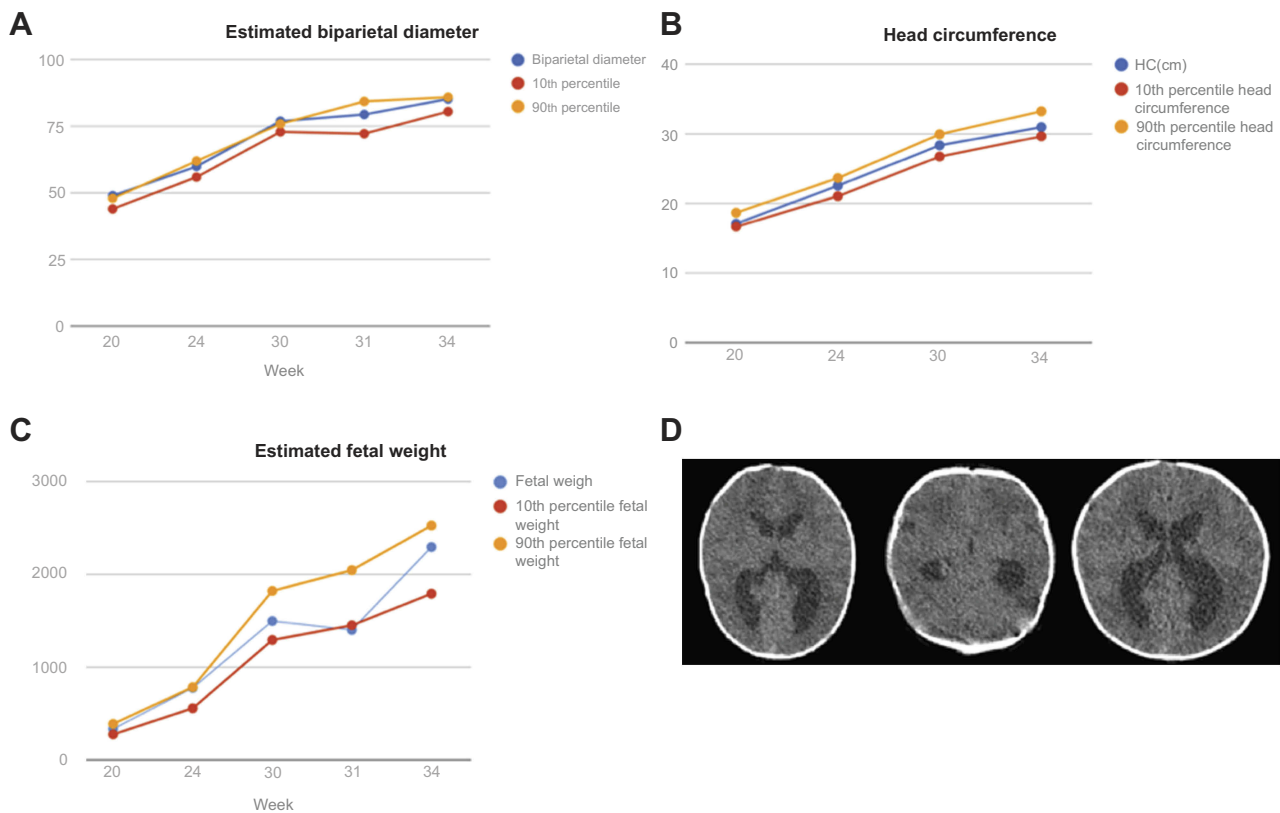
Figure 3 The different estimated measurements (estimated biparietal diameter, head circumference, estimated fetal weight) based on fetal ultrasonography records in five different measurements (20th, 24th, 30th, 31st and 34th week of gestation) Y-axis. Coaxial tomography scan (CT-scan) at 1 week after birth. Images correspond to the second case that involved hydrocephalus and clinical ventriculomegaly. (**A**) Representation of the different measurements of the biparietal diameter expressed in millimeters (mm) X-axis in a scatter plot. (**B**) Modeling the increase in head circumference expressed in centimeters (cm) X-axis at different time points by scatter plot. (**C**) Estimation of the fetal weight expressed in grams (**G**) X-axis at different points during gestation. The blue line represents different estimations (biparietal diameter, head circumference and fetal weight), the red line represents the 10th percentile in each parameter and the orange line represents the 90th percentile in each parameter (**D**). Post-natal ventriculomegaly demonstrated by coaxial tomography scan; the red arrows indicate the measurement of the lateral ventricular horn (measurement:16.2 mm) and the green arrows indicate asymmetric compensatory ventricular enlargement.

for ZIKV RNA, using TaqMan RT-PCR and quantitative RT-PCR for ZIKV following the CDC protocol. Means from standard methods were used to determine the levels of ZIKV IgM, IgG, and neutralizing antibody titers. We tested for other flaviviruses and arthropod-borne viruses. Additionally, the antibody levels of infectious diseases that can generate and cause congenital abnormalities such as cytomegalovirus, toxoplasma, syphilis, rubella, herpes, HIV, parvovirus B19, and hepatitis were tested in the mother and the newborn (Table 1). Additional details about the analyses are provided in the results section.

Karyotype and array comparative genomic hybridization

A blood karyotype analysis was performed after the pregnancy was terminated via the G-bending technique in classical cytogenetics. The karyotype analysis was performed using a microscope and the karyotype software

system Cytovision, with the cells in metaphase. Array CGH was performed on 1 mcg of DNA extracted from the peripheral blood cells of the patient using KaryoArray 3.0 (8×60K, Agilent) and was marked by fluorescence; the patient's DNA was compared with the control sample. DNA hybridization was performed with a human genomic microarray of 860 K oligonucleotides using commercially available Agilent-based arrays, which were analyzed using the Agilent scanner with Feature Extraction software (v9.1); statistically significant aberrations were determined using the aberration detection method 2 (ADM-2). The minimum number of following oligonucleotides to consider an alteration in the number of copies was three. For this reason, the medium resolution of the array was 1 oligonucleotide per 9 Kb in the regions of maximum interest, such as microdeletion/microduplication syndrome, telomeres, and centromeres. The algorithm in CGH Analytics version 3.5 was utilized (Agilent Technologies, Santa Clara, CA).[17]

Whole exome sequencing (WES)

The exome was captured using the 51 Mb SureSelect All Human Target Exon (Agilent's) capture kit and sequencing was performed using Illumina Hiseq 2,000 technology. During the sequencing, pairing readings of 101 nucleotides in size were obtained. The different variants were analyzed with a focus on genes related to the patient's phenotype and associated with microcephaly. A mutation appeared in WES and was discharged by Sanger sequencing.

Ethics and consent

Written informed consent was obtained from the patients' parents for publication of the case details and accompanying images. Data was collected following the Declaration of Helsinki Good Clinical Guidelines and protocol #253. This study was approved by the Ethics Committee of Fundación Valle del Lili (Act 11/2016).

Results

Autopsy and neuropathological findings

The fetal body from case one had a weight of 668 g (10th percentile), a length of 34 cm (10th percentile), and a circumference of 20 cm (less than −2 SD). The only obvious abnormality at the physical examination was microcephaly. The placenta weighed 100 g, resulting in a placenta: fetal weight ratio of 0.14 (<3rd percentile). A macroscopic examination of the CNS showed microcephaly (Figure 1A–E). The findings revealed almost complete agyria and internal hydrocephalus of the lateral ventricle. Full opening of the Sylvian fissures was observed, as were numerous and variable-sized calcifications in the cortex and subcortical white matter in all lobes (Figure 1A–E). Microscopic examination revealed lissencephaly (Figure 2A) and loosening of neural structures (Figure 2B). Perivascular infiltration of the lymphocytes was diffusely observed in the interstitial area (subcortical and white matter) converged into nests (Figure 2C), diffuse gliosis, secondary astrocyte reactivity, and multiple calcifications (Figure 2D), as well as the appropriate cytoarchitecture for the fetal brain.

The cerebellum, brain stem, and spinal cord showed no abnormalities, inflammation, degeneration, or calcifications. Wallerian degeneration of the brain stem was observed (Figure 2C). A histologic examination of the placental tissue showed focal calcifications in the villi and decidua, followed by umbilical cord thickening. There were no other relevant pathological findings in other fetal organs.

Molecular diagnosis

Serum and urine samples were tested for dengue virus, chikungunya virus, and ZIKV. The RT-qPCR for the dengue and chikungunya viruses was negative in all samples. The RT-qPCR for ZIKV confirmed the presence of ZIKV infection in the amniotic fluid of the patient but was negative in the urine and serum samples of the mother and fetus. Serology tests of the serum and urine using anti-dengue virus IgM, anti-dengue-virus IgG, anti-chikungunya-virus IgM and IgG, and anti-ZIKV displayed negative results in the ELISA. The samples were also negative for TORCHS (toxoplasmosis, HIV, syphilis, rubella, cytomegalovirus, herpes simplex 1 and 2, hepatitis, and parvovirus B19) (Table 1).

Karyotype and array CGH

Fetal karyotyping showed regular 46, XX and 46, XY (female and male) profiles, respectively. There were no losses and earnings of genomic material detected in the fetal DNA sample.

Whole exome sequencing

The WES did not detect either nucleotide variant in the sample to compare with the human reference template (GRCh38) or two mutation databases: Leiden Open (source) Variation Database (LOVD) and Human Gene Mutation Database.

Discussion

Zika became the first major infectious disease discovered in more than half a century that was linked to human birth defects.[5] In February 2016, the first case with an intrauterine transmission of the virus was reported. As a consequence of the infection, the fetus acquired neurological malformations.[18] At the end of the ZIKV outbreak, the risk of congenital neurologic defects related to ZIKV infection ranged between 6 and 42% in different reports.[14]

The spectrum of brain abnormalities described in the literature include microcephaly, cerebral calcifications, agenesis of vermis, Blake's pouch cyst, cerebral atrophy, mega cisterna magna and ventriculomegaly, thin or absent corpus callosum, abnormal gyration, vermian hypoplasia, asymmetric cerebral hemispheres, failure to develop the thalami, cerebellar hypoplasia, cortical and subcortical atrophy, arthrogryposis, and hydranencephaly. Currently, isolated hydrocephalus has not been published as a birth defect abnormality putatively associated with ZIKV infection; this

anomaly adds a better understanding of the dimension of Zika-related congenital brain abnormalities.[16,19–21]

In approximately one-third of cases, brain abnormalities were associated with evidence of cell migration abnormalities (eg, lissencephaly and pachygyria). Ventricular enlargement, secondary to cortical/subcortical atrophy, was also frequently reported. Excessive and redundant scalp skin, which was reported in 31% of cases, also suggests acute intrauterine brain injury, indicating arrest in cerebral growth but not in the growth of scalp skin.[22] Some cohorts presumed that severe and frequent problems in fetal and CNS development occurred in fetuses infected in the first trimester, but these findings suggested the pathologic change occurred during embryogenesis. However, brain abnormalities were also observed in fetuses infected as late as week 27 of gestation.[23]

The ZIKV embryopathy mimics a phenotype previously described in the literature: fetal brain disruption sequence (which is a recognizable pattern of birth defects consisting of severe microcephaly, overlapping sutures, prominence of the occipital bone, and scalp rugae). These manifestations develop after partial brain disruption, resulting in fetal skull collapse, which reduces the intracranial hydrostatic pressure and leads to severe microcephaly. This process is postulated to occur after 12 weeks of gestation due to a prenatal viral or parasitic infection and vascular disruption. This last cause might occur after environmental expositions to alcohol, tobacco, and radiation.[24,25] In the three cases reported by Russell et al (1984), there was clear evidence of marked cortical destruction, as was reported in our first case that had a similar phenotype as these patients, but without scalp fold and furrows.[25]

Some theories have been discussed regarding the possible effects of ZIKV in liver injury, particularly how it mediates the spillage of retinoid compounds and increases retinoic acid (RA) activation in hepatic cells. This process results in a high concentration of RA in the circulatory system and high retinaldehyde dehydrogenase (RD) activity. RD plays an essential role in the synthesis of RA from retinol and the spatial and temporal concentration of RA. RA is an essential factor of embryogenesis that acts as a morphogen in low concentrations and at high concentrations might be cytotoxic, pro-oxidant, mutagenic, and teratogenic. RA can bind its receptors in human DNA30, which are localized in several regulatory and promoter regions of different neural developmental genes. This mechanism could explain the broad spectrum of ZIKV congenital syndrome and its cerebral arrest[26]

After ZIKV infection, cholestatic liver damage occurs in early pregnancy due to activation of the retinoic cascade and interactions between the ZIKV genome and endogenous retinoid receptors (RAR) localized on hepatic stellate cells that mediate the liver injury and produce spillage of retinoid compounds in the liver. These compounds enter the systemic circulation, and the accumulative effect generates toxic concentrations. In this hypothesis, ZIKV genetically interacts with retinoic signaling by inducing RAR activation, as has been demonstrated with other viruses such as cytomegalovirus, hepatitis B virus, and HIV.[27] However, this theory does not explain the entire cerebral malformation spectrum that occurs in Zika microcephaly cases and liver injury is not a common feature of ZIKV syndrome. On the other hand, sequence homology exists between the ZIKV genome and the response elements of the early neural tube development marker (RA) in human DNA. Strains associated with microcephaly might dysregulate RA dependent genes by adding extra RARE consensus in the genome of the developing neural cells.[17] However, some evidence contradict this theory; 1. other viruses, such as dengue, can contain RARE in the genomic sequence; it is not exclusive to ZIKV. Thus, it cannot be associated with brain defect malformations. 2. Not all congenital ZIKV cases have calcifications that differ from isotretinoin embryopathy exposition during pregnancy. 3. Retinoic disruption defects are limited to brain development. However, arthrogryposis multiplex has been reported as part of the ZIKV syndrome spectrum. Further investigations must be performed focusing on testing the plausibility of this theory in animal models.

Microcephaly is an examination sign rather than an alethiological condition in which the cephalic perimeter is less than two standard deviations (SDs) from the mean for persons of this age and sex. This condition is typically associated with a smaller cerebral cortex.[28] The heterogeneous group of etiologies that generates microcephaly is characterized by brain growth failure due to injury in pattern formation, cell proliferation, differentiation, and survival.[28] These etiologies can be divided into three categories: gene mutations, chromosomal anomalies, and environmental damage. Intrauterine infection is the primary type of environmental damage, followed by exposure to teratogenic agents and hypoxic-ischemic injury.[24] Genetic causes remain diverse and are still increasing. In 2001, "microcephaly" produced almost 300 entries in the Online Mendelian Inheritance in Man database (http://www.ncbi.nlm.nih.gov/omim/), and when the updated

search was conducted, 1,302 results were obtained. The genes involved in congenital microcephaly play a crucial role in neural development and may also be involved in the evolutionary formation and conservation of the human cortex. Some of the genes described in the literature include LIS1, DCX, SHH, ZIC2, TGIF, SIX3, DHCR7, CREBBP, PAK3, NBS1, and MECP2.[28] Recent genetic analyses have identified five recessive microcephaly loci: the first is localized in chromosome 8p22-pter and contains the MCPH1 gene, the second is at 19q13.1–13.2 and contains the MCPH2 gene, the third and fourth are at 9q34 and 15q and contain the MCPH3 and MCPH4 genes, respectively, and the fifth is at 1q31 and contains the MCPH5 gene; other microdeletions include 16p13.3–12.1.[28] However, microcephaly can be part of several multiorgan genetic syndromes caused by chromosomal rearrangement, deletions, and monogenic diseases.[28]

Ventriculomegaly can be caused by a variety of disorders. It is defined as an atrial diameter greater than or equal to 10 mm, which is 2.5–4 SDs above the mean depending on the study.[29] Ventriculomegaly is considered isolated when the fetus has no other anomalies. The prevalence of ventricular enlargement is less than 2%,[30] but the condition is more prevalent in males. The principal causes of ventriculomegaly include idiopathic causes, chromosomal disorders and genetic syndromes, congenital infections, aqueductal stenosis, cortical malformations and migratory abnormalities.[31] In the cases we presented here, the only hazardous event during pregnancy was the ZIKV infection at the 10th and 17th weeks of gestation, respectively. We believe that the mechanism by which ZIKV causes brain abnormalities can lead to vascular disruption after 12 weeks of gestation due to the broad spectrum of fetal brain malformations.

Conclusion

In patients with microcephaly and/or brain abnormalities as a consequence of ZIKV perinatal infection, it is necessary to eliminate the possibility of other brain abnormality etiologies, such as maternal exposure to radiation, tobacco, drugs, and alcohol, and other perinatal infections present in countries with endemic infections for example; toxoplasma, CMV, and other infectious diseases. Additionally, many monogenic and chromosomal rearrangement disorders might contribute to the etiologies of these conditions. Therefore, a complete genetic study is mandatory, as is infection screening and a complete evaluation of the possible environmental expositions due to genetic disorders, which explain a vast number of microcephaly causes.

Author contributions

All authors contributed to data analysis, drafting and revising the article, gave final approval of the version to be published, and agree to be accountable for all aspects of the work.

Disclosure

The authors declare that the research was conducted in the absence of any commercial or financial relationships that could be construed as a potential conflict of interest.

References

1. Rodriguez-Morales AJ. Zika: the new arbovirus threat for Latin America. *J Infect Dev Ctries*. 2015;9:684–685. doi:10.3855/jidc.7230
2. Zika virus outbreaks in the Americas. *Releve Epidemiol Hebd*. 2015;90:609–610.
3. Fellner C. Zika virus: anatomy of a global health crisis. *Pharm Ther*. 2016;41:242–253.
4. Ventura CV, Maia M, Bravo-Filho V, Góis AL, Belfort R. Zika virus in Brazil and macular atrophy in a child with microcephaly. *The Lancet*. 2016;387:228. doi:10.1016/S0140-6736(16)00006-4
5. Petersen LR, Jamieson DJ, Powers AM, Honein MA. Zika virus. *N Engl J Med*. 2016;374:1552–1563. doi:10.1056/NEJMra1602113
6. Lanciotti RS, Kosoy OL, Laven JJ, et al. Genetic and serologic properties of Zika virus associated with an epidemic, Yap State, Micronesia, 2007. *Emerg Infect Dis*. 2008;14:1232–1239. doi:10.3201/eid1408.080287
7. Tognarelli J, Ulloa S, Villagra E, et al. A report on the outbreak of Zika virus on Easter Island, South Pacific, 2014. *Arch Virol*. 2016;161:665–668. doi:10.1007/s00705-015-2695-5
8. Brasil P, Calvet GA, Siqueira AM, et al. Zika virus outbreak in Rio de Janeiro, Brazil: clinical characterization, epidemiological and virological aspects. *PLoS Negl Trop Dis*. 2016;10:e0004636.
9. Butler D. First Zika-linked birth defects detected in Colombia. *Nature*. 2016;531(7593):153.
10. Pacheco O, Beltrán M, Nelson CA, et al. Zika virus disease in Colombia - preliminary report. *N Engl J Med*. 2016. doi:10.1056/NEJMoa1604037
11. Honein MA. Recognizing the global impact of Zika virus infection during pregnancy. *N Engl J Med*. 2018;378:1055–1056. doi:10.1056/NEJMc1711583
12. Posen HJ, Keystone JS, Gubbay JB, Morris SK. Epidemiology of Zika virus, 1947-2007. *BMJ Glob Health*. 2016;1:e000087. doi:10.1136/bmjgh-2016-000087
13. Chu V, Petersen L, Moore C. et al. Congenital Zika syndrome (CZS) phenotype seen in older children. *Open Forum Infect Dis*;2017. S696–S697. doi:10.1093/ofid/ofx163.1867
14. Hoen B, Schaub B, Funk AL, et al. Pregnancy outcomes after ZIKV infection in French territories in the Americas. *N Engl J Med*. 2018;378:985–994. doi:10.1056/NEJMc1711583

15. Candelo E, Caicedo G, Feinstein M, Pachajoa H. Microcefalia en Colombia antes de la epidemia del Zika: revisisi sistemmivis de la literatura. *Biomomtur*. 2018;38.

16. Mlakar J, Korva M, Tul N, et al. Zika virus associated with microcephaly. *N Engl J Med*. 2016;374:951–958. doi:10.1056/NEJMoa1600651

17. Blanco-Kelly F, Palomares M, Vallespín E, et al. Improving molecular diagnosis of aniridia and WAGR syndrome using customized targeted array-based CGH. *PLoS One*. 2017;12:e0172363. doi:10.1371/journal.pone.0172363

18. Oliveira Melo AS, Malinger G, Ximenes R, Szejnfeld PO, Alves Sampaio S, Bispo de Filippis AM. Zika virus intrauterine infection causes fetal brain abnormality and microcephaly: tip of the iceberg? *Ultrasound Obstet Gynecol*. 2016;47:6–7. doi:10.1002/uog.15831

19. Calvet G, Aguiar RS, Melo ASO, et al. Detection and sequencing of Zika virus from amniotic fluid of fetuses with microcephaly in Brazil: a case study. *Lancet Infect Dis*. 2016;16:653–660. doi:10.1016/S1473-3099(16)30197-9

20. Meaney-Delman D, Hills SL, Williams C, et al. Zika virus infection among U.S. Pregnant travelers. *MMWR Morb Mortal Wkly Rep*. 2016;65:211–214. doi:10.15585/mmwr.mm6508e1

21. Sarno M, Sacramento GA, Khouri R, et al. Zika virus infection and stillbirths: a case of hydrops fetalis, hydranencephaly and fetal demise. *PLoS Negl Trop Dis*. 2016;10:e0004517. doi:10.1371/journal.pntd.0004517

22. Schuler-Faccini L, Ribeiro EM, Feitosa IML, et al. Possible association between Zika virus infection and microcephaly - Brazil, 2015. *MMWR Morb Mortal Wkly Rep*. 2016;65:59–62. doi:10.15585/mmwr.mm6503e2

23. Brasil P, Pereira JP, Moreira ME, et al. Zika virus infection in pregnant women in Rio de Janeiro. *N Engl J Med*. 2016;375:2321–2334. doi:10.1056/NEJMoa1602412

24. Moore CA, Weaver DD, Bull MJ. Fetal brain disruption sequence. *J Pediatr*. 1990;116:383–386. doi:10.1016/S0022-3476(05)82825-2

25. Russell LJ, Weaver DD, Bull MJ, Weinbaum M. In utero brain destruction resulting in collapse of the fetal skull, microcephaly, scalp rugae, and neurologic impairment: the fetal brain disruption sequence. *Am J Med Genet*. 1984;17:509–521. doi:10.1002/ajmg.1320170213

26. De Kumar B, Parrish ME, Slaughter BD, et al. Analysis of dynamic changes in retinoid-induced transcription and epigenetic profiles of murine Hox clusters in ES cells. *Genome Res*. 2015;25:1229–1243. doi:10.1101/gr.184978.114

27. Mawson AR. Pathogenesis of zika virus-associated embryopathy. *Biores Open Access*. 2016;5:171–176. doi:10.1089/biores.2016.0004

28. Mochida G, Walsh C. Molecular genetics of human microcephaly. *Curr Opin Neurol*. 2001;14:151–156. doi:10.1097/00019052-200104000-00003

29. Farrell TA, Hertzberg BS, Kliewer MA, Harris L, Paine SS. Fetal lateral ventricles: reassessment of normal values for atrial diameter at US. *Radiology*. 1994;193:409–411. doi:10.1148/radiology.193.2.7972754

30. Clinical outcome of mild fetal ventriculomegaly - American Journal of Obstetrics & Gynecology [WWW Document], n.d. Available from: https://www.ajog.org/article/S0002-9378(98)80003-3/fulltext?code=ymob-site. Accessed June 22, 2018.

31. Scala C, Familiari A, Pinas A, et al. Perinatal and long-term outcomes in fetuses diagnosed with isolated unilateral ventriculomegaly: systematic review and meta-analysis. *Ultrasound Obstet Gynecol*. 2017;49:450–459. doi:10.1002/uog.15943